Research Article

Experiment and CFD Analysis of Reactive Muffler

[1]Yunshi Yao, [2]Shaodong Wei, [1]Jinpeng Zhao, [1]Shibin Chen, [1]Zhongxu Feng and [3]Jinxi Yue
[1]Key Laboratory for Highway Construction Technology and Equipment of Ministry of Education,
Chang'an University, Xi'an 710064, P.R. China
[2]China Orient Institute of Noise and Vibration, Beijing 100085, P.R. China
[3]XGMA Machinery Co., Ltd., Sanming 365500, P.R. China

Abstract: A conventional muffler used in vibratory rollers is usually designed based on experience and its performance could be enhanced in a large degree through structure optimization. In order to evaluate performance of reactive muffler and its effect on power loss of engine, flow field of muffler was discussed by CFD comparing with experimental test and the structure of reactive muffler was optimized. Based on results of simulation and optimization, the reactive muffler used in vibratory rollers with weight of 13t was fabricated and its field test was carried on. The simulate results showed that velocity field coincided with the pressure field basically, which indicates that the optimized muffler -2# has excellent aerodynamic characteristics and rational design of damping units. The results of field tests showed that 2# muffler had better acoustic insertion loss with little pressure loss. Acoustic insertion loss was 17~18.4 dB (A) at engine speed of 2450 rpm, which meets the designing goal.

Keywords: Acoustic insertion loss, computational fluid dynamics, flow field, pressure loss, reactive muffler

INTRODUCTION

The reactive muffler is an exhaust muffler which is most commonly used in the engines of the construction machines. The performance of the muffler affects the level of the machine's radiated noise and affects also the power loss of the engine. Many scholars have studied the exhaust muffler of automobiles or internal combustion engine and it was pointed that commercial automotive mufflers are often complex and difficult to be analyzed with predetermined transfer matrices (Panigrahi and Munjal, 2007).

In order to solve the problems of traditional exhaust silencers, such as poor noise reduction in low-frequency range and high exhaust resistance (Shao, 2011; Yasuda et al., 2013), research of muffler was conducted by simulation and experiment (Mimani and Munjal, 2011; Broatch et al., 2007). The simulating and experimental results show that internal flow field and sound field of the muffler were much complicated. The performance of the muffler affects not only the noise of the whole machine (Dias et al., 2007) and the sound quality of the interior of the cab (Wang et al., 2007; Shin et al., 2009), but also the power loss of the engine. With help of noise measurement and simulation analysis work, some new simulation approach was applied to evaluate the transient acoustic characteristics of exhaust muffler (Yasuda et al., 2010) and the

transmission loss of the muffler (Wu et al., 2008) and some new design methods were put out to increase effects of noise elimination for the mufflers (Lee and Jang, 2012). Besides sound transmission loss, the space-constrained condition must be taken into account (Chiu and Chang, 2008) and plug-inlet tube on a venting process by genetic algorithms is available for shape optimization of multi-chamber mufflers (Chiu, 2010).

Unlike the automobile engine, the engine of the construction machine has the features of relatively flat speed fluctuations, relatively rough load fluctuations and so on. Thus, the muffler of the construction machine cannot be the analogy of that of the automobile (Fang et al., 2009). It has an important value of engineering application for the simulating and optimal design and experimental study of the muffler.

The CFD has obvious advantages in the simulating and optimal design of the muffler and it can be used to obtain the dimensions of the acoustic muffler with the transmission loss, being maximized in the frequency range of interest (Barbieri and Barbieri, 2006). This study intends to conduct the simulating analysis and optimal design of the muffler for a vibratory roller and verifies it by the test, expecting to meet the needs of the practical engineering.

Corresponding Author: Yunshi Yao, Key Laboratory for Highway Construction Technology and Equipment of Ministry of Education, Chang'an University, Xi'an 710064, P.R. China
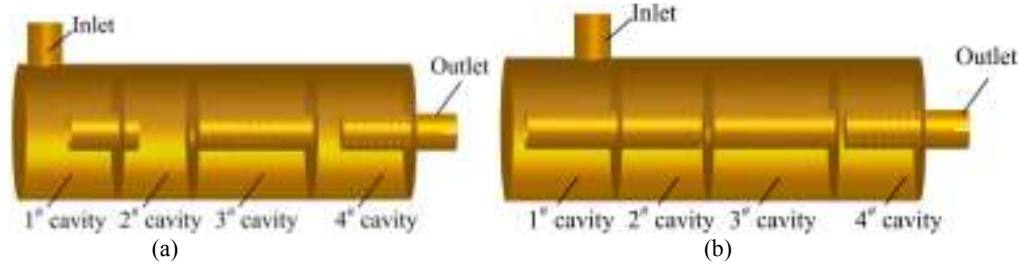
Fig. 1: The 3D models of the muffler (a) the 1# muffler, (b) the 2# muffler
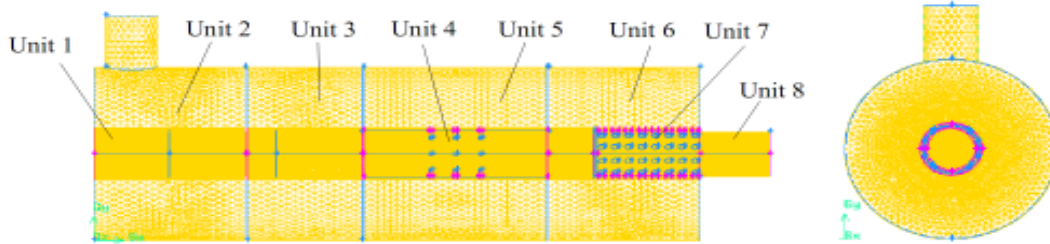

Fig. 2: The 3D grid model of the 2# reactive muffler

Table 1: The grid-dividing results of the muffler

Unit no	1# muffler		2# muffler	
	Spacing of the grids (mm)	Number of the units	Spacing of the grids (mm)	Number of the units
1	8	37684	8	37002
2	10	225689	10	232601
3	10	180529	10	207911
4	2.3	336966	2.3	349639
5	10	272349	10	272209
6	10	227439	10	196157
7	2.3	116937	2.3	119796
8	8	408697	8	415215

SIMULATION MODEL

Physical model: The structure and critical parameters were defined according to the spectral characteristics of the exhaust noise of a roller. The 3D models of the 1# muffler without optimization and the 2# muffler with optimization were conducted using Pro-E software, of which were transformed into Step file, as shown in Fig. 1.

Dividing the model grids: The grids of models were divided by the processing software named by Gambit and were output into Mesh format. The grids used non-structural tetrahedron and were divided some blocks and there were no overlaying surfaces in adjacent volumes of each block. The model of the muffler was divided into 8 blocks, using the unit grids of Tet/Hybrid and T Grid, as shown in Fig. 2. The results of the dividing grids are listed in Table 1.

Setting the initial and boundary conditions: The initial and boundary conditions are the premise that the fluid control equation has exact solutions. Its inlet conditions, outlet conditions, wall surface conditions and initial conditions need to be defined when the fluid dynamics of the reactive muffler was analyzed using the Fluent software. Considered the actual running parameters of a roller, the initial and boundary conditions are as follows:

Inlet Temperature: 735K
The Density of Air: $0.47 kg/m^3$
Specific heat capacity at constant pressure: 1071J/(kg/K)
Thermal Conductivity: 0.05638w/(m/K)
Kinetic Viscosity: $3.56×10-6$ Pa·s
Prandtl Number: 0.685 Pa·s
The Material of the Muffler: Q235-steel
Wall surface temperature: 423K
Adiabatic, no friction and no slip
The Approximate Inlet Air Speed of the Muffler: 41 m/s

Choosing the inlet boundary condition of the speed, the turbulence intensity is 0.043 and the relative pressure outside is 0Pa. Choosing the boundary condition of the pressure outlet, the turbulence intensity is the same with that of the inlet. And the outlet temperature of the 1# and 2# mufflers are respectively 518 K and 521 K.

Model simplification: Considering the calculation and the needs of engineering practice comprehensively,
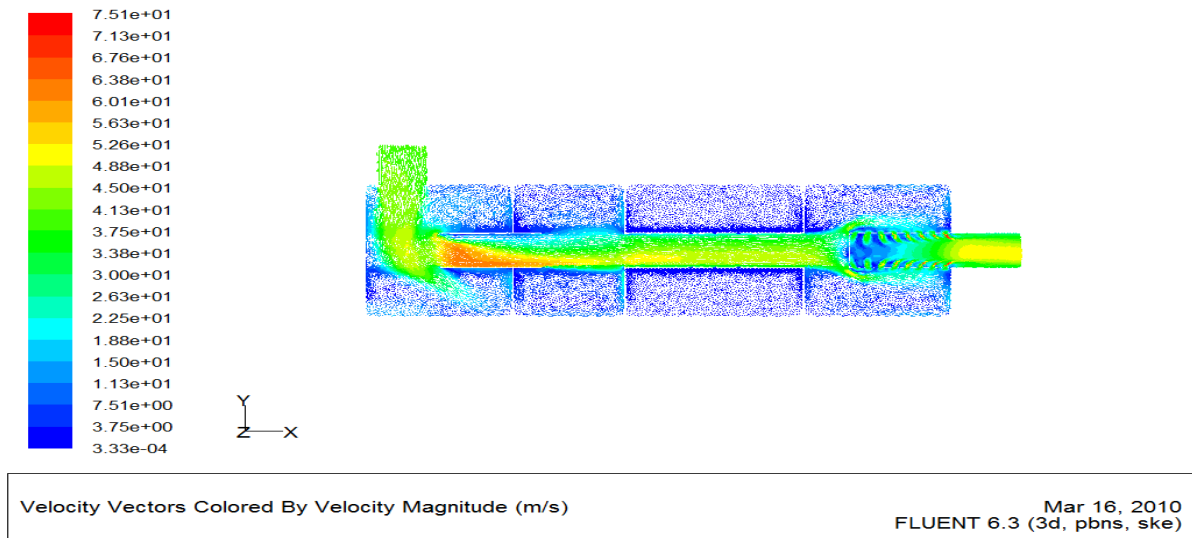
(a)
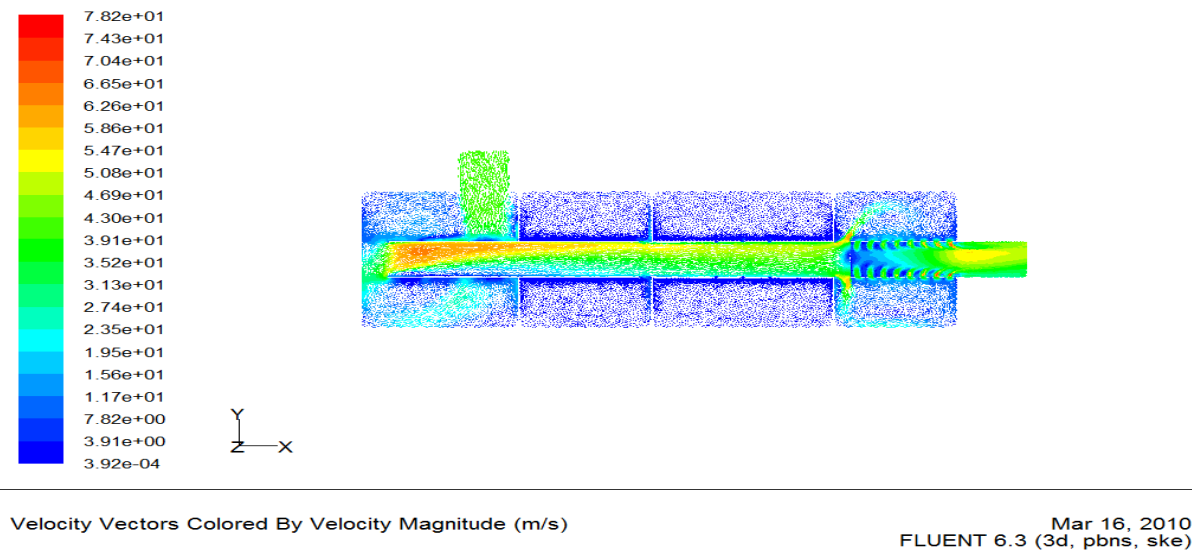
(b)

Fig. 3: The distribution of the velocity sector (a) the 1# muffler, (b) the 2# muffler

some simplifications are made as follows: The flow of the fluid is a fixed-length and incompressible turbulence; The gravitational field is out of consideration; The inlet velocity of flow of the muffler is uniform and the effects of pulsation is out of consideration; The solid wall is adiabatic during the calculation of convective heat transfer with no friction and no slip.

SIMULATION AND ANALYSIS

Using the software-Fluent to calculate with standard k-ε turbulence-model.

The velocity vector and the distribution of the velocity field: As can be known from Fig. 3 to 4, the overall trend of airflow and tendency of all mufflers are basically the same, which flows into the first cavity with high speed through the inlet, then it fleetly flows into the second cavity after the buffer of the expansion chamber and it flows into the third cavity quickly after some buffer in a degree in the second expansion chamber (the effect of buffer of the airflow isn't as obvious as it in the first expansion chamber because the length of the cavity and the tube are short with an axial arrangement), after some frictional speed reduction through a long straight tube, it enters the forth cavity. In the forth chamber, the flow goes through expanding buffer and baffle shunt reduction firstly, then it enters the outlet tube after going through the perforated pipe in the forth cavity. Finally, the airflow flows out after being accelerated by the outlet tube.
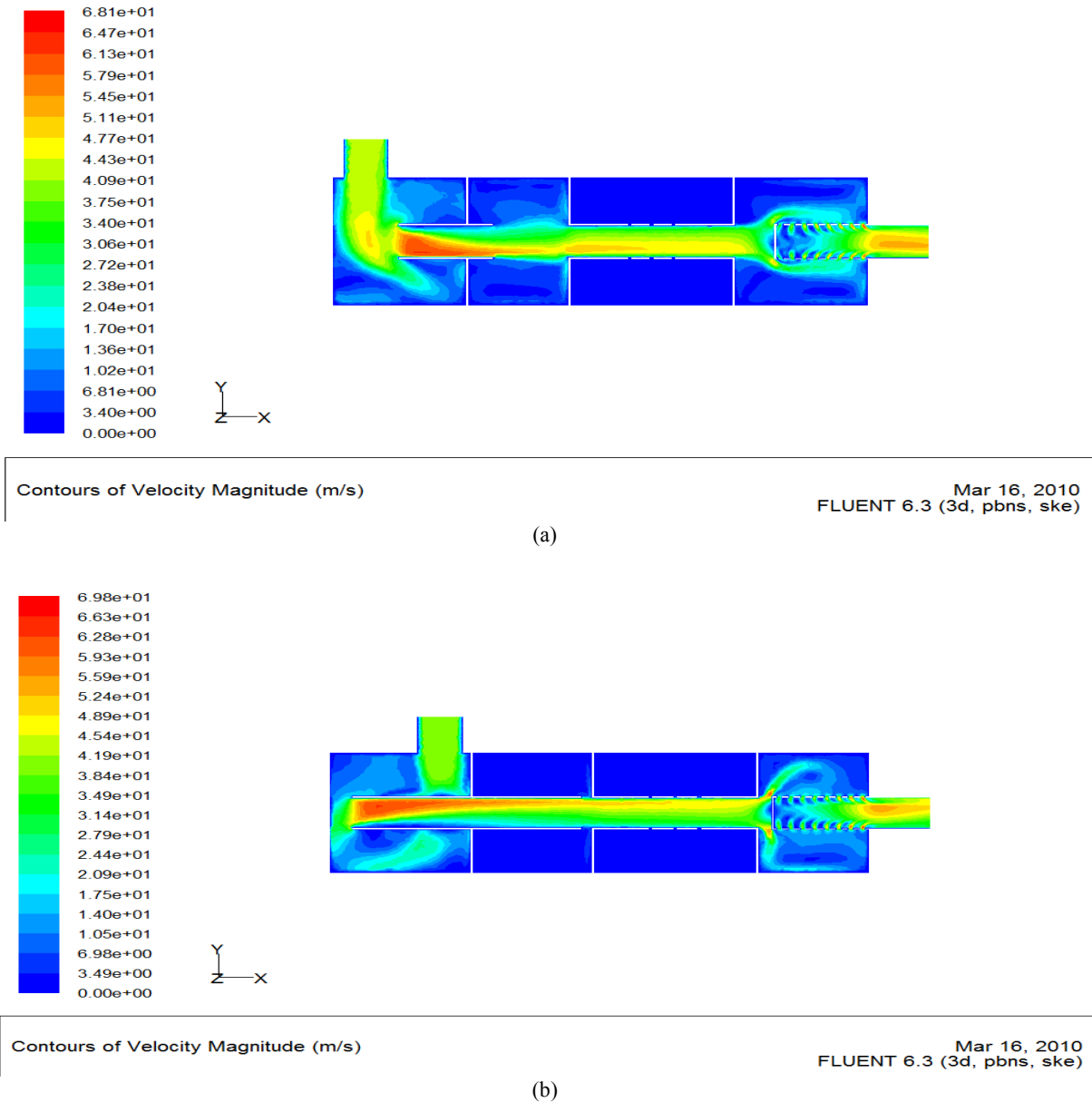
(a)

(b)

Fig. 4: The distribution of the velocity field (a) the 1# muffler, (b) the 2# muffler

Partial flow differences are raised due to the differences in the structure of all mufflers. The airflow of which the velocity is about 41 m/s in the inlet place of 1# muffler produces obvious eddy after entering the first cavity in the expansion chamber. And the velocity of the flow in the core of the whirling is up to 52 m/s. Then the unordered flow goes through the first intubation and arises crash and impact on the inside wall of the tube opposite to the inlet, which leads to great velocity gradients along the longitudinal section of the intubation. On one side, the highest flow speed is about 63 m/s, on the other side, the lowest flow speed is only about 30 m/s. The airflow continues expanding after entering the second chamber for the reason that

the first intubation is too short. And the highest flow speed falls to 48 m/s, the velocity gradient continues to fall further while the speed gap is about 8 m/s. When the airflow arrives to the outlet of the third cavity, it produces eddy in small scopes with the speed in the core being about 51 m/s. As the flow goes through the third chamber, its speed falls to 41 m/s further. Finally, it flows out accelerate through the forth chamber and the perforated pipe. At the outlet, the flow shows features that the speed in the core is high while it is low around. Also, there are great velocity gradients in it. The core flow speed is up to about 51 m/s while the speed near the wall of the tube is lower, only about 41 m/s. Compared with the airflow of the 1# muffler, the
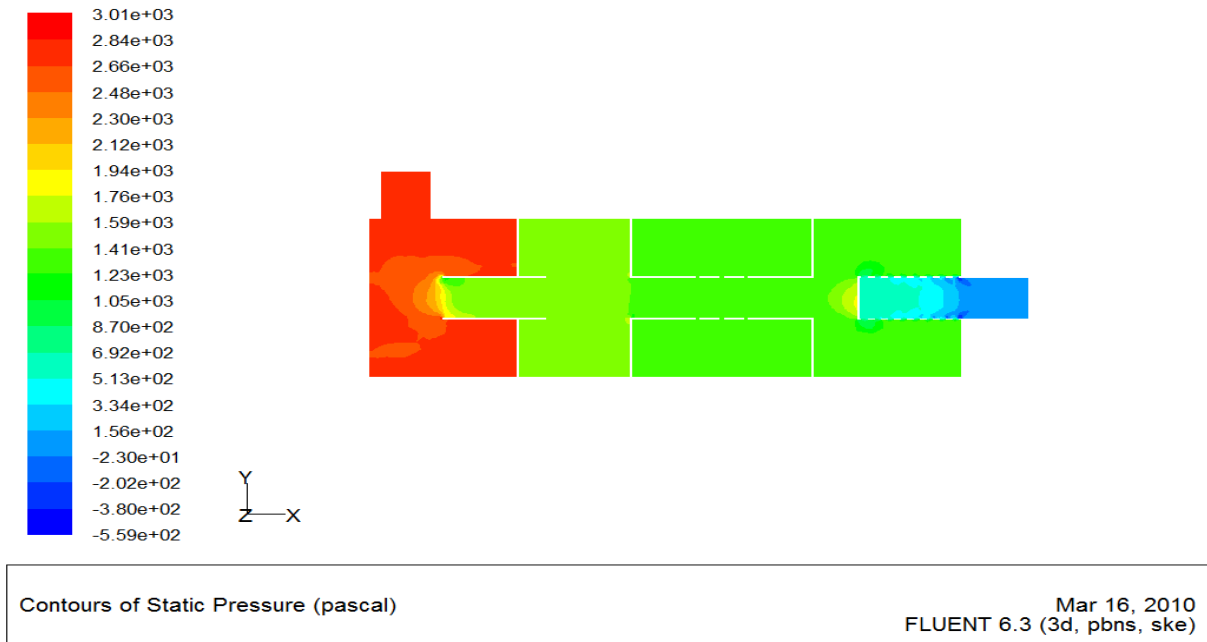
(a)
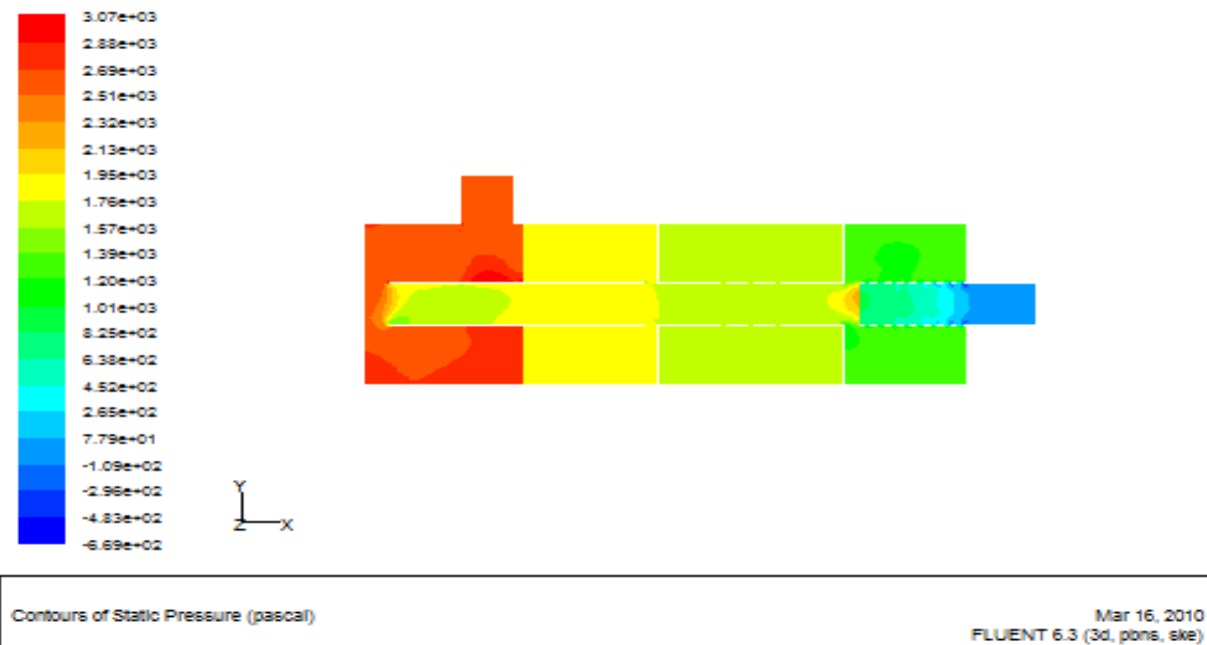
(b)

Fig. 5: The distribution of the static pressure field (a) the 1# muffler, (b) the 2# muffler

flow at the rate of about 41 m/s of the 2# muffler has no such obvious whirling after entering the first cavity through the inlet. The direction of the flow changes while the speed falls smoothly from the highest speed of about 62 m/s to the rate of 49 m/s at the inlet of the forth cavity after it suffered crash and impact on the one side of the first intubation. Finally, the flow rushes out with high speed after being accelerated by the forth chamber and the perforated pipe, the core speed of the

Table 2: The highest flow speed of the flow field inside the muffler and its corresponding mach number

Muffler	1#	2#
Highest airflow speed (m/s)	63.0	61.6
Mach number	0.11	0.11

flow is about 52 m/s while it is about 49 m/s near the walls of the tube with no obvious velocity gradients. Comparatively speaking, the speed of the flow inside the 2# muffler is evener and more stable with less

Table 3: The pressure loss of the mufflers

Muffler	Average static pressures of inlets (Pa)	Average dynamic pressures of inlets (Pa)	Average static pressures of outlets (Pa)	Average dynamic pressures of outlets (Pa)	Pressure losses (Pa)
1#	2746.5	409.8	66.3	508.9	2581.1
2#	2599.8	373.8	-31.0	489.2	2515.4

Table 4: The experimental results on the scene

Rotational speeds of engine(rpm)	Temperature of the outlets (°C)			Insertion losses (dB(A))		Air speeds of the outlets (m/s)	
	Blank pipe	1# muffler	2# muffler	1# muffler	2# muffler	1# muffler	2# muffler
770	164	148	161	11.6~12.8	11.5~13.0	7	10
1400	186	156	180	14.5~17.5	15.6~8.4	11.6	21.6
1700	190	164	181	16.2~16.8	16.2~17.8	15.8	26.6
2000	211	180	199	16.0~17.7	16.2~18.5	20.3	33.8
2200	226	198	213	16.5~17.1	17.4~18.5	25.7	34.1
2450	271	213	231	15.7~16.5	17.0~18.4	31.5	44.7

impact to the walls of the cavity, also, with better flowing effect of the air.

The highest speed of the flow field inside all the mufflers and the corresponding Mach number is shown as Table 2. All the Mach Number which have the highest flow speed inside the mufflers are less than the critical mach-0.3 MPa between the compressible and the uncompressible, which indicates that it is practical to take the airflow as uncompressible flow during the flow-field -simulating calculation.

The distribution of the static pressure: From Fig. 5, the static pressure at the inlet of the front intubation in the first cavity of the 1# muffler and the static pressure in the first chamber have no obvious decrease, which indicates that the buffer effect of the first cavity on the airflow is little and this is a primary reason for the rise of the whirlings in the first chamber. The static pressure has a relatively great change when the flow enters the third chamber, which is primarily due to the fact that there is obvious divergence when the flow enters the third cavity and it then gives rise to the flow to contribute crash and impact to the wall sides near the outlet of the second chamber and this has distractions on noise elimination. The static pressure at the inlet of the front intubation in the first cavity of the 2# muffler decreases obviously comparing to that at the inlet and in the first chamber, which indicates that the first cavity has great buffer effects on the airflow. Secondly, the flow has relatively small change in static pressure when it enters the third chamber from the second chamber of the 2# muffler. Thus it can be seen that the analysis result of the static pressure field are basically the same as that of the speed field and the static pressure changes in the flow fied inside the 2# muffler are relatively more stable and the pressure distribution is evener comparing with that in the 1# muffler.

The average static and dynamic pressures at the inlet and outlet of all mufflers can be obtained after measuring and analyzing the measuring points inside the flow field of the muffler and the pressure loss of all the mufflers can be obtained after correction computation, which can be shown as Table 3. From Table 3, the pressure loss of the 2# muffler is less than

Table 5: The comparison between the experimental and simulating results of the outlet air speed

Mufflers	Experimental results on the scene (m/s)	Simulating-calculating results(m/s)
1#	31.5	41.7
2#	44.7	49.4

that of the 1# muffler, while the aerodynamic and structural quality are better than the latter's.

TEST AND ANALYSIS

The results and analysis of the test: The test can value the optimal l effect of the muffler more accurately and validate the validity of the simulating analysis. The method of contrast test of the 1# muffler without optimization and the 2# muffler with optimization has been adopted. And the A-weighted sound pressure level, 1/3 octave band sound pressure levels as well as the level of the air speed at the exhaust pipe end are measured through referring to the national standards-The Measuring Methods of the exhaust Muffler in the Engine GB/T4759-2009-to value the noise eliminating and pressure loss. The experimental results are shown as Table 4.

From Table 4, at all rotational speeds, the outlet temperature of blank pipe is the highest and then is the 2# mufflers and the 1# muffler's is the lowest. The outlet temperature of the 2# muffler is higher than that of the 1# muffler by about 13-24°C; the insertion loss of the 2# muffler is obviously higher than that of the 1# muffler by about 1~2 dB (A) averagely. The insertion loss of the 2# muffler is 17~18.4dB (A) when the rotational speed of the diesel engine is 2450 r/min. And the air speed at the outlet of the 2# muffler is commonly higher than that of the 1# muffler, which indicates that the aerodynamic quality and structure of the 2# muffler are better with more insertion loss and less pressure loss.

Comparison of test and simulation: The results of comparing the observed outlet air speed with the CFD simulation of the muffler are shown as Table 5.

From Table 5, the simulating results and the observed results have some differences, which are primarily because some simplifications have been

conducted during the simulation. However, the differences between the simulating results and the observed results have no effect on the basic laws of the muffler's flow field, therefore the qualities of the 1# and 2# mufflers can be basically valued. This indicates that the CFD simulating method in this study is basically right.

CONCLUSION

This study conducted the optimal design and the test on a reactive muffler of a vibratory roller based on the CFD and experimental study. The results of the study are as follows:

- The simulating results of the velocity field basically tally with those of the pressure field, which indicates that the aerodynamic quality of the 2# muffler optimized is better and the structure of the noise eliminating units is much reasonable
- The results of the real vehicle test indicate that the 2# muffler optimized has more insertion loss and less pressure loss and the insertion loss is up to 17~18.4 dB (A) which fits the goal of the design when the rotational speed of the diesel engine is 2450 r/min
- There have been some differences between the simulating results and the observed results due to the simplifications conducted on the simulating model. However, this can still reflect the basic laws of the muffler's flow field before and after its optimization, which indicates that the CFD simulating method in this study is basically right.

ACKNOWLEDGMENT

REFERENCES

Barbieri, R. and N. Barbieri, 2006. Finite element acoustic simulation based shape optimization of a muffler. Appl. Acoust., 67(4): 346-357.

Broatch, A., J.R. Serrano, F.J. Arnau and D. Moya, 2007. Time-domain computation of muffler frequencyresponse:Comparison of different numerical schemes. J. Sound Vib., 305(1-2): 333-347.

Chiu, M.C., 2010. Shape optimization of multi-chamber mufflers with plug-inlet tube on a venting process by genetic algorithms. Appl. Acoust., 71(6): 495-505.

Chiu, M.C. and Y.C. Chang, 2008. Numerical studies on venting system with multi-chamber perforated mufflers by GA optimization. Appl. Acoust., 69(11): 1017-1037.

Dias, T., R. Monaragala and E. Lay, 2007. Analysis of thick spacer fabrics to reduce automobile interior noise. Meas. Sci. Technol., 18(7): 1979-1991.

Fang, J.H., Y.Q. Zhou, X.D. Hu and L. Wang, 2009. Measurement and analysis of exhaust noise from muffler on an excavator. Int. J. Precis. Eng. Man., 10(5): 59-66.

Lee, J.W. and G.W. Jang, 2012. Topology design of reactive mufflers for enhancing their acoustic attenuation performance and flow characteristics simultaneously. Int. J. Numer. Meth. Eng., 91(5): 552-570.

Mimani, A. and M.L. Munjal, 2011. Transverse plane wave analysis of short elliptical chamber mufflers: An analytical approach. J. Sound Vib., 330(7): 1472-1489.

Panigrahi, S.N. and M.L. Munjal, 2007. A generalized scheme for analysis of multifarious commercially used mufflers. Appl. Acoust., 68(6): 660-681.

Shao, Y.L., 2011. A study on exhaust muffler using a mixture of counter-phase counteract and split-gas rushing. Proc. Eng., 15: 4409-4413.

Shin, S.H., J.G. Ih, T. Hashimoto and S. Hatano, 2009. Sound quality evaluation of the booming sensation for passenger cars. Appl. Acoust., 70(2): 309-320.

Wang, Y.S., C.M. Lee, D.G. Kim and Y. Xu, 2007. Sound-quality prediction for nonstationary vehicle interior noise based on wavelet pre-processing neural network model. J. Sound Vib., 299(4-5): 933-947.

Wu, C.J., X.J. Wang and H.B. Tang, 2008. Transmission loss prediction on a single-inlet/double-outlet cylindrical expansion-chamber muffler by using the modal meshing approach. Appl. Acoust., 69(2): 173-178.

Yasuda, T., C. Wu, N. Nakagawa and K. Nagamura, 2010. Predictions and experimental studies of the tail pipe noise of an automotive muffler using a one dimensional CFD model. Appl. Acoust., 71(8): 701-707.

Yasuda, T., C. Wu, N. Nakagawa and K. Nagamura, 2013. Studies on an automobile muffler with the acoustic characteristic of low-pass filter and Helmholtz resonator. Appl Acoust., 74(1): 49-57.